Role of iron and TfR1 in the application of high dose ascorbate against pancreatic cancer

Alban Piotrowsky, Christian Leischner, Hendrik Schmieder, Katja Detert, Kathrin Schneider, Johanna Schulte, Sabrina Hammerschmidt, Luigi Marongiu, Olga Renner, Markus Burkard, Sascha Venturelli

Angaben zur Veröffentlichung / Publication details:

Piotrowsky, Alban, Christian Leischner, Hendrik Schmieder, Katja Detert, Kathrin Schneider, Johanna Schulte, Sabrina Hammerschmidt, et al. 2026. "Role of iron and TfR1 in the application of high dose ascorbate against pancreatic cancer." *Oncology Reports* 55 (4): 78. https://doi.org/10.3892/or.2026.9083.

Role of iron and TfR1 in the application of high-dose ascorbate against pancreatic cancer

ALBAN PIOTROWSKY[1], CHRISTIAN LEISCHNER[1], HENDRIK SCHMIEDER[1], KATJA DETERT[1], KATHRIN SCHNEIDER[2,3], JOHANNA SCHULTE[1], SABRINA HAMMERSCHMIDT[1], LUIGI MARONGIU[1], OLGA RENNER[4], MARKUS BURKARD[1,5] and SASCHA VENTURELLI[1,6]

[1]Department of Nutritional Biochemistry, Institute of Nutritional Sciences, University of Hohenheim, D-70599 Stuttgart, Germany; [2]Bavarian Center for Cancer Research (BZKF), D-86156 Augsburg, Germany; [3]Pathology, Medical Faculty, University of Augsburg, D-86156 Augsburg, Germany; [4]Hochschule Niederrhein, University of Applied Sciences, Faculty of Food and Nutrition Sciences, D-41065 Moenchengladbach, Germany; [5]Department of Internal Medicine VIII, Medical Oncology and Pneumology, University Clinic Tuebingen, D-72076 Tuebingen, Germany; [6]Department of Vegetative and Clinical Physiology, Institute of Physiology, University of Tuebingen, D-72074 Tuebingen, Germany

Received October 16, 2025; Accepted February 2, 2026

DOI: 10.3892/or.2026.9083

Abstract. Pancreatic cancer remains one of the deadliest tumor diseases with an urgent need for new therapy options. At the same time, the use of high-dose vitamin C in cancer treatment has been investigated for decades. Despite promising *in vitro* and *in vivo* data and initial clinical studies, there is a need for optimization with regard to an ideal treatment regimen and suitable patient population for the use of high-dose vitamin C. The aim of the present study was to evaluate for the first time the combination of high-dose vitamin C with the administration of iron in three human pancreatic cancer cell lines and to determine the exact cell death mechanism. While the investigated cell lines showed a high susceptibility to ascorbate treatment, the combination treatment with $FeCl_3$ generally led to a reduction in the ascorbate effect and in the formation of reactive oxygen species. The ascorbate-induced cell death showed no signs of apoptosis but clear ferroptotic properties. Furthermore, treatment of the tumor cells with $FeCl_3$ was accompanied by reduced expression of TfR1, preventing an increase in the intracellular labile iron pool. The present study provided valuable information on the mechanism of action of high-dose vitamin C in pancreatic cancer, whereby a combination treatment with ferric iron in the context of tumor therapy is not recommended based on these data.

Correspondence to: Dr Markus Burkard or Professor Sascha Venturelli, Department of Nutritional Biochemistry, Institute of Nutritional Sciences, University of Hohenheim, Garbenstrasse 30, D-70599 Stuttgart, Germany
E-mail: markus.burkard@uni-hohenheim.de
E-mail: sascha.venturelli@uni-hohenheim.de

Abbreviations: AM, acetoxymethyl ester; BIP, 2',2'-bipyridyl; BSA, bovine serum albumin; CQ, chloroquine; DAPI, diamidino-2-phenylindole; DCFH-DA, dichlorodihydrofluorescein diacetate; DFO, deferoxamine mesylate; FCS, fetal calf serum; GPX4, glutathione peroxidase 4; HRP, horseradish peroxidase; LIP, labile iron pool; MUH, 4-methylumbeliferyl heptanoate; PI, propidium iodide; RAPA, rapamycin; ROS, reactive oxygen species; RSL3, RAS-selective lethal 3; STS, staurosporine; TCA, trichloroacetic acid; TBH, tert-butyl hydroperoxide; TBST, Tris-buffered saline containing 0.1% Tween-20; TfR1, transferrin receptor 1

Key words: ascorbate, vitamin C, pancreatic cancer, pancreatic ductal adenocarcinoma, iron, ROS, TfR1

Introduction

Pancreatic tumors are one of the deadliest malignancies. In 2024, they were the third most deadly tumor entity, despite ranking 10th in cancer incidence (1). A further increase in pancreatic tumor-related deaths is expected in the coming years, so that it is predicted to rank second within a few years (2). Of all pancreatic tumors, pancreatic ductal adenocarcinoma (PDAC) is the most common and also the most fatal (3). While life expectancy for numerous other tumor diseases has increased significantly thanks to improvements in therapy options, hardly any progress has been made in this regard for PDAC, with an average 5-year survival rate of 13% despite current standard therapy (4).

The use of high-dose vitamin C (ascorbic acid or ascorbate), so-called pharmacological ascorbate, in tumor therapy has been the subject of medical research for several decades, starting with Linus Pauling's and Ewan Cameron's findings on increased survival when treating tumor patients with high-dose ascorbate (5,6). However, it was only numerous years later that it became clear that the plasma ascorbate concentrations required for antitumor efficacy can only be achieved by intravenous administration (up to ~25 mM) (7), but not by oral intake (up to ~0.2 mM) (8).

High-dose ascorbate has been investigated as a monotherapy or combination therapy for various tumor entities in a large number of studies. The majority of preclinical studies have focused on the use of ascorbate in leukemia, colorectal carcinoma, melanoma, and PDAC and have consistently shown that high-dose ascorbate reduces the viability of tumor cells and decreases tumor size in animals, as nicely summarized by Böttger *et al* (9). With regard to pancreatic cancer, an *in vitro* study by Kim *et al* (10) reported that high-dose ascorbate as monotherapy reduces the proliferation and survival of PDAC cells by inhibiting glucose metabolism. In addition, high-dose ascorbate suppressed the invasion and metastasis of PDAC cells (10). The effects of high-dose ascorbate on tumor cells are also reflected in studies carried out *in vivo*. In mice with PDAC tumors, a reduction in tumor growth (42%), metastasis, and ascites formation and also an improvement in the survival rate were achieved with high-dose ascorbate (11). A recent randomized clinical trial also provides evidence that supplementing standard therapy with high-dose ascorbate prolongs the survival time of PDAC patients (12).

Overall, the use of high-dose ascorbate is considered safe and well tolerated, as has been observed in several human studies (13-16). Chen *et al* (14) investigated the pharmacokinetics and safety of intravenously administered vitamin C with increasing doses in healthy individuals and cancer patients. The plasma ascorbate concentration of >5 mM (equivalent to 88 mg/dl), which is toxic for various cancer cell lines, could already be achieved with infusions of 25 g vitamin C. No side effects were observed in the participants in the present study, in which cardiac and liver function as well as metabolic and coagulation parameters were examined (14). In other studies, however, mild side effects such as nausea, vomiting, headache, and discomfort at the injection site were described. Severe side effects can occur in patients with glucose-6-phosphate dehydrogenase deficiency. This condition therefore represents a contraindication for therapy with high-dose ascorbate (17).

Ascorbate has both antioxidant and pro-oxidant properties. Which of these properties predominates depends, among other things, on the local ascorbate concentration and the presence of transition metals. At plasma concentrations in the micromolar range, as achieved through diet or oral supplementation, ascorbate has predominantly antioxidant functions, for example, as a radical scavenger (18). However, if pharmacological concentrations in the millimolar range are present, as can be achieved by intravenous administration, ascorbate can serve as a pro-drug for the formation of hydrogen peroxide (H_2O_2), which is necessary for the pro-oxidant effect (19,20). Catalytic metal ions play a decisive role in ascorbate-induced H_2O_2 formation, particularly free iron (so-called labile iron), which increases H_2O_2 formation as part of the Fenton reaction. Compared with healthy cells, cancer cells have larger amounts of redox-active labile iron, so that high ascorbate concentrations increase its pro-oxidative properties, which explains the selective cytotoxicity of high-dose ascorbate towards tumor cells (17,21). For this reason, an involvement of the transport protein transferrin receptor 1 (TfR1), which mediates cellular iron uptake in its trivalent form, in the antitumor ascorbate effect is also suspected (22).

In recent years, there has been growing evidence of increased cytotoxicity of high-dose ascorbate against tumor cells in combination treatment with various iron compounds based on this mechanism of action. While simultaneous treatment with iron and ascorbate appears to be counterproductive in this context and neutralizes the ascorbate effect, several studies show a successful increase in treatment efficacy when high-dose ascorbate is used after prior iron treatment (23-25). Although in all three of these publications iron was used as a preincubation prior to ascorbate treatment, different iron compounds were used: While Piotrowsky *et al* (23) used 100 μM ferric chloride, Zhou *et al* (24) used ferrous ammonium sulphate (100 μM) as well as ammonium ferric citrate (100 μM), and Schoenfeld *et al* (25) used ferrous ammonium sulphate (100 μM or 250 μM). There are also initial findings in PDAC cells, where iron in the form of iron-hydroxyquinoline was used (26). However, the question of the success of such a form of combination treatment with other iron compounds in pancreatic carcinoma remains unanswered in order to investigate the general validity of the recommendation for combination treatment.

For this reason, the aim of the present study was to investigate whether a combination treatment of iron and high-dose ascorbate also leads to increased cytotoxicity against various human pancreatic cancer cell lines. In addition, it should be investigated whether the TfR1 expression in the tumor cells allows conclusions to be drawn about the susceptibility to high-dose ascorbate treatment.

Materials and methods

Cell culture and reagents. The human pancreatic carcinoma cell lines BxPC-3, MIA PaCa-2, and PANC-1 were obtained from the German Collection of Microorganisms and Cell Cultures (DSMZ). All cell lines were cultured in RPMI-1640 medium (MilliporeSigma-Aldrich, cat. no. R0883) with 10% fetal calf serum (FCS, MilliporeSigma-Aldrich, cat. no. F7524) and 1% penicillin/streptomycin (MilliporeSigma-Aldrich, cat. no. P4333) at 37˚C and 5% CO_2. HPDE6c7 cells were obtained from MilliporeSigma-Aldrich (cat. no. SCC442) and cultured in EpiVita Growth Medium for adult keratinocytes (MilliporeSigma-Aldrich, cat. no. 141-500A) with 1% penicillin/streptomycin, 50 μg/ml endothelial cell growth supplement from bovine pituitary (MilliporeSigma-Aldrich, cat. no. E0760) and 5 ng/ml epidermal growth factor (MilliporeSigma-Aldrich, cat. no. SRP3027) at 37˚C and 5% CO_2. All cell lines tested negative for mycoplasma infection.

Ascorbate (Pascorbin®) was purchased from Pascoe pharmazeutische Praeparate GmbH (CAS: 50-81-7, cat. no. 00150343). Staurosporine (STS; CAS: 62996-74-1, cat. no. HY-15141) and RAS-selective lethal 3 (RSL3; CAS: 1219810-16-8, cat. no. HY-100218A) were obtained from MedChemExpress. Chloroquine (CQ) and rapamycin (RAPA) were obtained from Enzo Biochem, Inc. (ENZ-51031). Triton™ X-100, tert-butyl hydroperoxide (TBH), and 4-methylumbeliferyl heptanoate (MUH) were purchased from MilliporeSigma-Aldrich (Triton™ X-100: CAS 9002-93-1, cat. no. T8787; TBH: CAS 75-91-2, cat. no. 416665; MUH: CAS 18319-92-1, cat. no. M2514). Deferoxamine mesylate (DFO) was obtained from Selleck Chemicals LLC (cat. no. S5742).

Cell viability measurement. To determine cell viability, the MUH assay was performed as previously described (23). The cells were seeded in 24-well plates, according to their proliferation behavior, at a cell density of $2x10^4$ (PANC-1), $3x10^4$ (MIA PaCa-2), or $4x10^4$ (BxPC-3) cells per well. Depending on the planned experiments, $FeCl_3$ was added to the medium at a final concentration of 100 μM during seeding. 24 h after seeding, the medium was discarded, the cells were washed twice with PBS and treated with the indicated ascorbate concentrations for a further 24 h. Triton™ X 100 served as a positive control.

To perform the MUH assay, the medium was discarded, the cells were washed once with PBS and the MUH reagent was added in phenol red-free, FCS-free RPMI-1640 medium (100 μg/ml). After an 1-h incubation period at 37˚C, the fluorescence intensity at 460 nm was measured which is proportional to the number of living cells using the Synergy™ H1 microplate reader (BioTek Instruments, Inc.). From this, the relative percentage of living cells in relation to the untreated control was calculated.

Immunoblotting. A total of $1x10^5$ (PANC-1), $1.5x10^5$ (MIA PaCa-2), or $2x10^5$ (BxPC-3) cells were seeded in 6-well format and incubated for 24 h. To determine basal protein expression, cell lysis was performed afterwards as described below. For the experiments with iron, $FeCl_3$ was added at different concentrations during seeding and subsequently cell lysates were generated. Afterwards, the cells were either lysed as described later (to investigate the influence of iron on protein expression) or, to investigate the influence of ascorbate treatment on protein expression, the medium was changed 24 h after seeding and the cells were treated with different ascorbate concentrations for 6 h. A total of 10 μM STS served as a positive control for apoptosis, 5 μM RSL3 as a positive control for ferroptosis, and 60 μM CQ with 500 nM RAPA as a positive control for autophagy. For the untreated control, the medium was also changed, but without any added treatment. After treatment, the cells were washed twice with PBS and lysed on ice by adding 50 μl of lysis buffer [150 mM NaCl, 50 mM Tris-HCl, pH 7.4, 1% Triton™ X-100, 0.5% sodium deoxycholate, 0.1% sodium dodecyl sulfate (SDS), 10 μl/ml aprotinin, 10 μl/ml leupeptin, 10 μl/ml pepstatin A, 1.5 μl/ml PMSF, and 1 μl/ml Na_3VO_4]. After incubation on ice for 30 min, cell debris was removed from the lysates by centrifugation at 16,200 x g at 4˚C for 20 min and transferring the supernatant to a new reaction tube. The lysates were stored at -20˚C until further use. The protein concentration of the lysates was determined using the Lowry method. From each lysate, 35 μg protein was mixed with Laemmli buffer (250 nM Tris-HCl pH 6.8, 40% glycerol, 8% SDS, 20% 2-mercaptoethanol, crumb bromophenol blue) and boiled at 95˚C for 5 min. The proteins were then separated by electrophoresis in a 10 or 15% SDS polyacrylamide gel. The proteins were subsequently transferred to a PVDF membrane, blocked for 1 h at RT in 5% milk powder in Tris-buffered saline containing 0.1% Tween-20 (TBST) and incubated overnight at 4˚C with the following primary antibodies [diluted at 1:1,000 in 5% bovine serum albumin (BSA, cat. no. 8076.1, Carl Roth GmbH & Co.)]: anti-Cleaved Caspase-3 (cat. no. ab2302; Abcam), anti-Glutathione peroxidase 4 (GPX4; cat. no. 52455), anti-TfR1 (cat. no. 13113) anti-GAPDH (cat. no. 2118) or anti-LC3B (cat. no. 2775; all from Cell Signaling Technology, Inc.). The next day, incubation with the secondary antibody [goat anti-rabbit IgG, horseradish peroxidase (HRP)-coupled: cat. no. 7074s; 1:10,000 in 5% milk powder in TBST; Cell Signaling Technology Inc.] in 5% milk powder solution in TBST was carried out at RT for 45 min. After washing three times with TBST, the proteins were analyzed by adding the WesternBright chemiluminescence substrate Sirius (Biozym Scientific GmbH) in the Fusion FX chemiluminescence detector (Vilber). The densitometric evaluation was performed using ImageJ version 1.54r. (National Institutes of Health).

Reverse transcription-quantitative PCR (RT-qPCR). The cell lines were seeded in the previously mentioned cell numbers in 6-well format and incubated for 24 h at 37˚C and 5% CO_2. In the case of iron treatment, 100 μM $FeCl_3$ was added to the medium at seeding. This was followed by RNA isolation using the Quick-RNA™ Miniprep Kit (Zymo Research Corp.) according to the manufacturer's protocol. Subsequently, 1 μg of RNA per sample was used for cDNA synthesis using the iScript cDNA Synthesis Kit (Bio-Rad Laboratories, Inc.) according to the manufacturer's instructions. The SYBR® Green RT-PCR Reaction Mix (Bio-Rad Laboratories, Inc.) and the following primer pairs were used for qPCR: TfR1 forward, 5'-ATTGAA CCTGGACTATGAGAG-3' and reverse, 5'-TGGAAGTAG CACGGAAGA-3'; GAPDH forward, 5'-GGTCGGAGTCAA CGGATTTG-3' and reverse, 5'-GGAAGATGGTGATGGGAT TTC-3'. The qPCR program in the CFX96 Touch Real-Time PCR Detection System (Bio-Rad Laboratories, Inc.) was composed as follows: 2 min at 95˚C and 40 cycles with 10 sec at 95˚C, 30 sec at 58˚C, and 30 sec at 72˚C. The $2^{-\Delta\Delta Cq}$ method was used to calculate the relative gene expression of TfR1 as described by Livak and Schmittgen (27).

Fluorescence microscopy. The cells were seeded in the aforementioned cell numbers in 24-well format on cover slips. After 24 h of treatment, the medium was changed and the cells were treated with different ascorbate concentrations for 6 h. Treatment with 5 μM STS (apoptosis) or 1 μM RSL3 (ferroptosis) served as a positive control. After treatment, the cells were washed once with PBS and fixed by adding 4% PFA in PBS for 20 min. They were washed again with PBS and quenched with 150 mM glycine in PBS for 10 min. After a further washing step, phalloidin staining was performed. For this, the cells were stained with phalloidin tetramethylrhodamine B isothiocyanate (Phalloidin-TRITC, cat. no. P1951, 10 μg/ml in PBS; MilliporeSigma-Aldrich) for 1.5 h at RT. The cells were washed once with PBS and stained with diamidino-2-phenylindole (DAPI, cat. no. 6335.1, Carl Roth GmbH & Co.) solution (1:1,000 in PBS) for 20 min in the dark. After washing again with PBS and double-distilled water, the cells were mounted on slides with mounting medium (Fluoromount-G®, cat. no. 0100-01, SouthernBiotech). Fluorescence images were captured with a Lionheart FX fluorescence microscope (BioTek Instruments, Inc.).

Cell cycle analysis. Cell cycle analysis was performed to detect apoptosis as previously described (23). The cells were seeded in the aforementioned cell numbers per cell line in 6-well format and incubated for 24 h. Subsequently, the medium was changed, and the cells were treated with different ascorbate

concentrations for 24 h. Treatment with 1 μM or 20 μM STS for 20 h served as a positive control. After treatment, the cells were harvested by trypsinization, washed once with PBS, and fixed by adding 70% ice-cold ethanol at 4˚C overnight. The cells were then washed twice with PBS and incubated in PBS with 50 μg/ml propidium iodide (PI, cat. no. P4170, Sigma-Aldrich; Merck KGaA) and 100 μg/ml RNAse (cat. no. 10109142001, Roche Diagnostics) at 4˚C for 20 min. This was followed by flow cytometric analysis of the cell cycle phases (NovoCyte® 2060R flow cytometer, Agilent Technologies,). A total of 10,000 events per sample were recorded and three independent experiments were performed.

Intracellular reactive oxygen species (ROS) measurement. To analyze intracellular (ROS) levels, the dichlorodihydrofluorescein diacetat (DCFH-DA) assay was performed as previously described (28). Cells were seeded in the aforementioned cell numbers in 24-well format with or without the addition of 100 μM $FeCl_3$. A total of 24 h after seeding, cells were washed twice with PBS and treated with different ascorbate concentrations or 500 μM TBH as a positive control for 6 h. After treatment, the cells were harvested by trypsinization and the cell pellet was washed twice with PBS. This was followed by incubation with 5 μM DCFH-DA (cat. no. D6883, MilliporeSigma-Aldrich) in phenol red-free, FCS-free RPMI-1640 medium at 37˚C in the dark for 30 min. The cells were then pelleted again and washed once with PBS, resuspended in phenol red-free, FCS-free RPMI, and analyzed by flow cytometry (NovoCyte® 2060R flow cytometer; Agilent Technologies, Inc.). With absorbance at 488 nm and detection of emission at 530 nm, 10,000 events per sample were recorded and three independent experiments were performed.

Quantification of the labile iron pool. To measure the intracellular labile iron pool (LIP), the calcein acetoxymethyl ester (AM) assay was performed as described by Schönfeld *et al* (25). The cells were seeded in the aforementioned cell numbers in 24-well format. During seeding, $FeCl_3$ was added to the cells at different concentrations. A total of 24 h after seeding, the cells were harvested by trypsinization, washed twice with PBS, and incubated after addition of PBS with 500 nM calcein AM (cat. no. C1359, MedChemExpress) for 15 min at 37˚C in the dark. The cells were pelleted, washed once more with PBS, and resuspended in PBS. The cell suspension was divided into two flow cytometry tubes and 2',2'-bipyridyl (BIP) was added to one of these tubes per treatment at a final concentration of 100 μM. After a 15 min incubation at RT in the dark, the cells were analyzed by flow cytometry (NovoCyte® 2060R flow cytometer; Agilent Technologies, Inc.) with absorbance at 488 nm and emission measurement at 515 nm. The relative LIP was determined by subtracting the mean fluorescence intensity without BIP addition from the mean fluorescence intensity with BIP and normalizing the result to the untreated control. For each sample, 10,000 events were recorded and three independent experiments were performed.

Statistical analysis. The statistical data analysis and the calculation of IC_{50} values were performed with GraphPad Prism version 10.4.1 (GraphPad Software, Inc.; Dotmatics). For multiple group comparisons, one-way ANOVA with subsequent Dunnett's multiple comparisons test was used for P-value calculation and significance determination. $P \leq 0.05$ was considered to indicate a statistically significant difference.

Results

Effect of high-dose ascorbate alone and in combination with iron on the viability of pancreatic cancer cells. The MUH assay was performed to investigate the cytotoxic effect of high-dose ascorbate and its combination treatment with ferric chloride on human pancreatic cancer cells. While no cytotoxicity was observed after 24 h of treatment at the concentration of 0.2 mM (achievable in plasma by oral supplementation), treatment with pharmacological ascorbate concentrations (only achievable by intravenous administration) led to a rapid decrease in relative cell viability in all cell lines investigated (Fig. 1A). While the BxPC-3 cells proved to be the most resistant cell line with a significant reduction of the number of viable cells from 0.8 mM ascorbate and an IC_{50} of 0.89 mM, a significant cytotoxic effect on the MIA PaCa-2 and PANC-1 cells occurred from 0.4 mM onwards, with IC_{50} values of 0.43 mM (MIA PaCa-2) and 0.45 mM (PANC-1), respectively. In all three cell lines analyzed, the relative cell viability dropped to below 20% at 2 mM ascorbate at the latest.

Two different approaches were investigated for the combination treatment of ascorbate and iron. In the co-incubation with $FeCl_3$, the treatment was carried out simultaneously with both substances (Fig. 1B). In this case, the combination treatment led to a complete inhibition of ascorbate-induced cytotoxicity. This was true for all cell lines analyzed as well as for all concentrations used.

In the preincubation with iron, the 24 h ascorbate treatment followed a previous treatment for 24 h with 100 μM $FeCl_3$ (Fig. 1C). In this case, the influence of the combination treatment varied depending on the cell line. In BxPC-3 cells, the combination treatment with 0.8 and 1 mM ascorbate led to a significantly greater decrease in cell viability than ascorbate treatment alone (0.8 mM: 78% vs. 63%, 1 mM: 52% vs. 36%). In the MIA PaCa-2 cells, none of the analyzed concentrations differed significantly between combination treatment and ascorbate treatment alone. On the other hand, the PANC-1 cells showed an inhibition of the ascorbate effect in the concentrations 0.8 and 1 mM by combination treatment with preincubated $FeCl_3$ (0.8 mM: 23% vs. 51%, 1 mM: 18% vs. 35%).

To increase the transferability of the results, the experiments were performed in the form of preincubation with holo transferrin instead of $FeCl_3$ for all three cell lines (Fig. S1). Consistent with the data on preincubation with $FeCl_3$, treatment with holo transferrin only led to a slight increase in efficacy when BxPC-3 cells were treated with 2 mM ascorbate, while no effect on treatment efficacy was observed in MIA PaCa-2 and PANC-1 cells.

Investigation of apoptosis as a possible ascorbate-induced cell death mechanism. To detect possible apoptosis as an ascorbate-induced cell death mechanism, caspase-3 cleavage after treatment was analyzed by flow cytometry (Fig. 2A) and western blotting (Fig. 2B). Neither method was able to detect any activation of caspase 3 after 6 h of treatment for any of

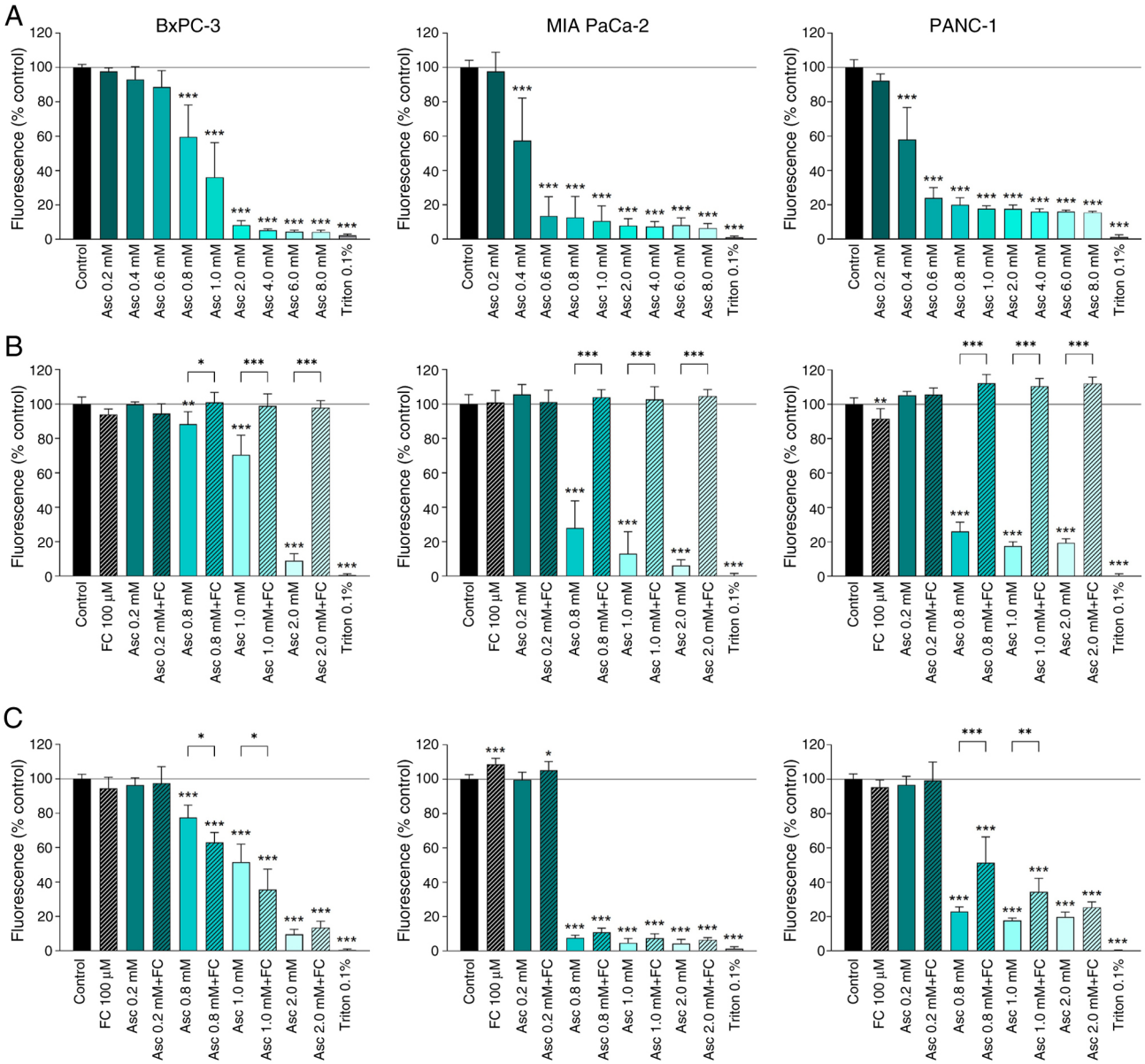

Figure 1. Influence of high-dose ascorbate alone or in combination with ferric iron on the viability of human pancreatic cancer cell lines. The cell lines BxPC-3, MIA PaCa-2 and PANC-1 were either treated for 24 h with the indicated ascorbate concentrations alone (A), in the form of coincubation simultaneously with ascorbate and 100 μM FC (B), or incubated with 100 μM FC for 24 h as a preincubation before ascorbate treatment (C). Triton™ X-100 at 0.1% (v/v) served as positive control. Cell viability was measured after treatment by MUH assay. The results are presented as a percentage of fluorescence intensity relative to the untreated control. Three independent experiments were performed in duplicates. Error bars represent the mean ± SD, statistical analysis with one-way ANOVA and subsequent Dunnett's multiple comparisons test, confidence interval 95%. *P≤0.05, **P≤0.01, and ***P≤0.001. Asc, ascorbate; FC, ferric chloride; MUH, 4-methylumbelliferyl heptanoate.

the ascorbate concentrations or cell lines analyzed. This also applied to ascorbate concentrations that led to a decrease in cell viability to below 20% in the MUH assay.

As a further indication of possible apoptotic ascorbate-mediated cell death, apoptosis-typical nuclear fragmentation was examined using fluorescence staining (Fig. 2C). While ascorbate treatment visibly reduced the phalloidin staining of the filamentous actin, no apoptotic cell nuclear fragmentation could be detected in any of the cell lines examined due to the highly cytotoxic ascorbate concentration of 2.0 mM and thus no evidence of apoptotic cell death was found here either.

To confirm these results, a flow cytometric cell cycle analysis was performed by PI staining after ascorbate treatment (Fig. 2D). In agreement with the previous results, no increase in the SubG1 fraction as an indication of apoptosis-typical DNA fragmentation was observed in the BxPC-3 cell line. In the MIA PaCa-2 and PANC-1 cells, a significant increase in the SubG1 fraction was evident at the highest ascorbate concentration (2 mM) analyzed. However, the lower ascorbate concentrations of up to 1 mM, which also caused a decrease in cell viability of at least 80%, similarly provided no evidence of apoptotic cell death.

Evaluation of ferroptosis as an ascorbate-induced cell death mechanism. Based on the hypothesized main mechanism of action of high-dose ascorbate in cancer cells, ferroptotic cell

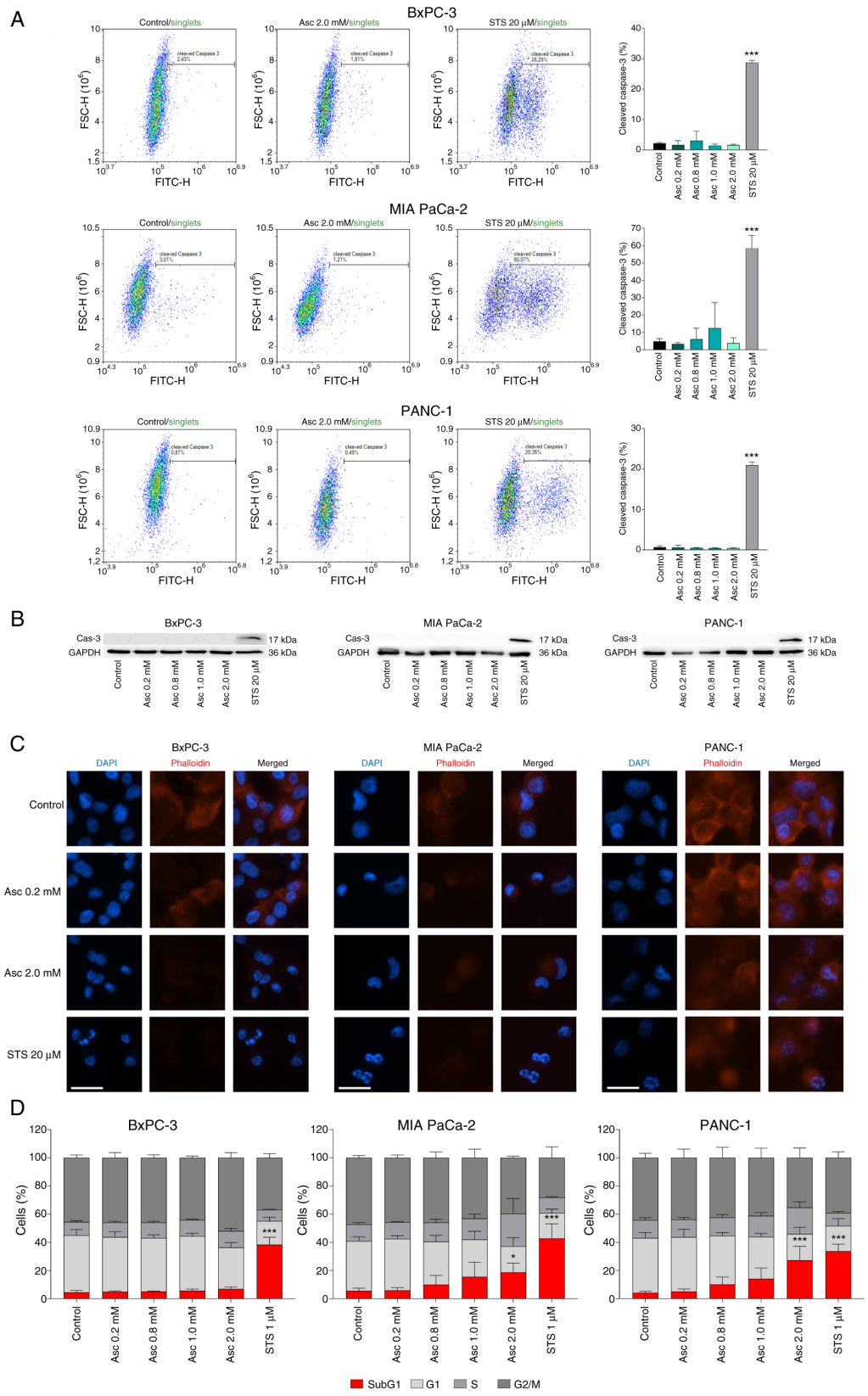

Figure 2. Investigation of the effect of high-dose ascorbate treatment on different apoptosis markers in human pancreatic cancer cell lines. A possible induction of apoptosis in the human pancreatic cancer cell lines BxPC-3, MIA PaCa-2, and PANC-1 was investigated by testing caspase-3 cleavage by flow cytometry (A) and western blotting (B). Cells were treated for 6 h with the indicated ascorbate concentrations. 20 μM STS served as positive control. Three independent experiments were performed. Morphological nuclear changes were detected by fluorescence microscopy. The white scale bars represent 25 μm. (C). Cells were treated with the indicated ascorbate concentrations for 6 h and then fixed. 10 μM STS served as positive control. The nuclei were stained with DAPI (blue), the cytoskeleton with phalloidin (red). A representative experiment is shown. Cell cycle analysis was performed by flow cytometry (D). Cells were treated with the indicated ascorbate concentrations for 24 h, fixed, stained with PI, and subsequently detected. Treatment with 1 μM STS for 20 h served as positive control. Three independent experiments were performed. Error bars represent the mean ± SD, statistical analysis with one-way ANOVA and subsequent Dunnett's multiple comparisons test, confidence interval 95%. *P≤0.05 and ***P≤0.001. Asc, ascorbate; DAPI, diamidino-2-phenylindole; PI, propidium iodide; STS, staurosporine.

death is often suspected in this context (23,29). For this reason, ferroptotic cell death following ascorbate treatment was evaluated by investigating the effect of the ferroptosis inhibitor DFO (Fig. 3A). In BxPC-3 and PANC-1 cells, the addition of DFO to the treatment at all effective ascorbate concentrations led to a significant, in some cases complete suppression of the ascorbate effect, which was reflected in a lower decrease in cell viability in the MUH assay. In the MIA PaCa-2 cells, DFO also had a strong inhibitory effect at ascorbate concentrations of 0.8 and 1 mM. At 2 mM, however, ascorbate cytotoxicity predominated and DFO only led to a slight, non-significant inhibition of the treatment effect.

Further indications of ferroptosis are increased TfR1 expression and reduced expression of the antioxidant active enzyme GPX4 (30). Therefore, both parameters were also analyzed by western blotting (Fig. 3B). In addition, the expression of both proteins was analyzed densitometrically (Fig. 3C). In order to detect autophagy in the tumor cells, which is another feature of ferroptotic cell death (30), LC3B-II expression was also examined after ascorbate treatment.

While increased TfR1 expression was observed in the BxPC-3 cells starting at 0.8 mM 6 h ascorbate treatment, the MIA PaCa-2 and PANC-1 cells showed reduced expression as a result of treatment. GPX4 expression was significantly reduced in all three cell lines after ascorbate treatment, in the MIA PaCa-2 cells and PANC-1 cells even at the lowest ascorbate concentration of 0.2 mM, strongly indicating ferroptotic cell death. In agreement with these results, a clear induction of autophagy was observed in all three cell lines, as indicated by increased LC3B-II expression. Ascorbate treatment in the MIA PaCa-2 cells led to the strongest increase in LC3B-II expression, followed by the PANC-1 and finally the BxPC-3 cells, reflecting the sensitivity of the different cell lines to high-dose ascorbate.

Influence of iron on ROS induction of high-dose ascorbate and TfR1 expression. Based on the observed signs of ferroptotic cell death after ascorbate treatment with simultaneous reduction of the ascorbate effect by combination with iron, the influence of 24 h iron treatment on ascorbate-induced ROS formation (DCFH-DA assay) as well as intracellular LIP (calcein AM assay) and TfR1 expression (western blotting and qPCR) was investigated (Fig. 4). While ascorbate treatment alone led to a concentration-dependent increase in intracellular ROS levels in all cell lines, co-incubation with 100 μM ferric chloride simultaneously with ascorbate treatment resulted in a significant and almost complete inhibition of intracellular ROS formation in the pancreatic cancer cell lines (Fig. 4A).

By contrast, preincubation with 100 μM ferric chloride for 24 h and subsequent ascorbate treatment showed a significant increase in intracellular ROS levels in BxPC-3 and PANC-1 cells from 0.8 mM. However, in MIA PaCa-2 cells, no difference in ROS induction was observed between ascorbate treatment alone and ascorbate treatment after prior iron preincubation (Fig. 4B).

The influence of a 24 h incubation with ferric chloride on the LIP of pancreatic cancer cells was investigated using the calcein AM assay (Fig. 4C). In BxPC-3 cells, all concentrations analyzed resulted in a reduction of the LIP that reached significance at 100 μM. The MIA PaCa-2 and PANC-1 cells, on the other hand, showed no significant change in the LIP due to iron treatment.

The basal expression of TfR1 in the three pancreatic cancer cell lines and in the non-malignant human pancreatic ductal epithelial cell line HPDE6c7 was determined by western blotting and quantified densitometrically (Fig. 4D). Interestingly, HPDE6c7 cells showed almost no detectable TfR1 protein expression, whereas the most ascorbate-sensitive cell line MIA PaCa-2 showed the highest expression, followed by BxPC-3 and PANC-1 cells. Furthermore, the influence of 24 h iron treatment on TfR1 expression was analyzed by western blotting and qPCR to find a possible explanation for the observations relating the LIP (Fig. 4E). Ferric chloride treatment led to a significant reduction in TfR1 expression, with an almost complete inhibition of protein expression being observed in the BxPC-3 cells both at the mRNA and protein level. By contrast, treatment with the highest orally achievable ascorbate concentration had no effect on TfR1 mRNA expression in BxPC-3 and PANC-1 cells. Gene expression increased slightly in MIA PaCa-2 cells, but this increase was also not significant.

Discussion

To the best of our knowledge, the present study is the first to investigate the antitumor efficacy of a combination treatment of high-dose ascorbate and iron in pancreatic cancer cells. Despite the general assumption that the effect of ascorbate against tumor cells is mainly based on ROS induction involving intracellular labile iron (9), the combination treatment in the present model did not lead to an increase in cytotoxicity, on the contrary even to a decrease in efficacy in most cases. While simultaneous treatment with ascorbate and iron also led to a reduction in cytotoxicity in other tumor entities in previous studies, the treatment regimen of preincubation often resulted in increased potency (23,31,24). In glioblastoma, for example, increased ascorbate-induced cytotoxicity was shown *in vitro* after prior incubation of the cells with $FeCl_3$ (23). The same has been shown *in vitro* with colon carcinoma cells and in osteosarcoma (31,24).

However, in a recent study on prostate cancer cells, Deme *et al* (32) also showed a reduction in the effect of ascorbate after preincubation of the cells with $FeCl_3$ for 24 h prior to ascorbate treatment. These partly contradictory data suggest that the benefit of iron may be tumor entity-specific. The mutation of the KRAS gene could play a role here. For example, the cell lines mentioned, in which preincubation with iron led to an increase in the ascorbate effect, predominantly carry the KRAS wild-type gene. In the present study, too, the only cell line in which at least a slight increase in ascorbate cytotoxicity could be achieved was a KRAS wild-type cell line. By contrast, the cell lines in which preincubation with $FeCl_3$ had the opposite effect were KRAS-mutated cells. On the other hand, the increased overall sensitivity of KRAS-mutated cancer cells is described in the clinical phase III study by Wang *et al* (33) on the use of high-dose ascorbate in metastatic colorectal cancer. While the addition of high-dose ascorbate to the treatment regimen FOLFOX (leucovorin, 5-fluorouracil, and oxaliplatin) and bevacizumab showed no benefit on progression-free survival, objective response rate, and overall

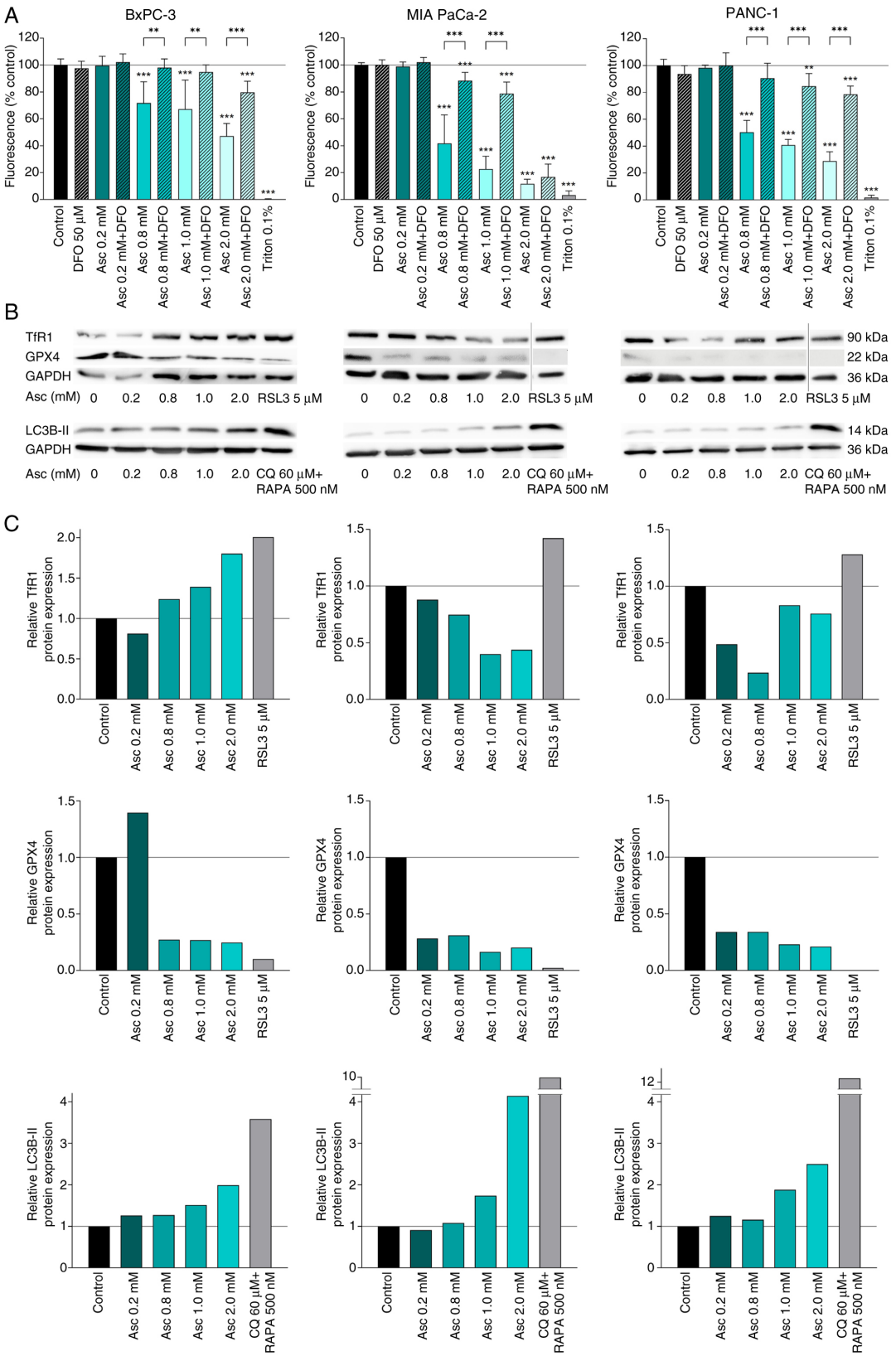

Figure 3. Investigation of the effect of high-dose ascorbate treatment on different ferroptosis markers in human pancreatic cancer cell lines. The human pancreatic cancer cell lines BxPC-3, MIA PaCa-2, and PANC-1 were treated with or without the ferroptosis inhibitor DFO for 24 h, after which cell viability was measured using the MUH assay (A). Triton™ X-100 at 0.1% (v/v) served as positive control. The results are presented as a percentage of the fluorescence intensity of the untreated control. Three independent experiments were performed in duplicates. As further signs of ferroptosis, protein expression of TfR1, GPX4, and LC3B-II was detected by western blotting (B) and quantified densitometrically (C). Cells were treated with the indicated ascorbate concentrations for 6 h, after which a western blot was performed. 5 μM RSL3 or 60 μM CQ together with 500 nM RAPA were used as positive controls. Signal intensity was analyzed densitometrically and normalized to GAPDH. One representative experiment out of two is shown. Error bars represent the mean ± SD, statistical analysis with one-way ANOVA and subsequent Dunnett's multiple comparisons test, confidence interval 95%. **P≤0.01 and ***P≤0.001. Asc, ascorbate; CQ, chloroquine; DFO, deferoxamine mesylate; GAPDH, glyceraldehyde 3-phosphate dehydrogenase; GPX4, glutathione peroxidase 4; MUH, 4-methylumbelliferyl heptanoate; RAPA, rapamycin; RSL3, RAS-selective lethal 3; TfR1, transferrin receptor 1.

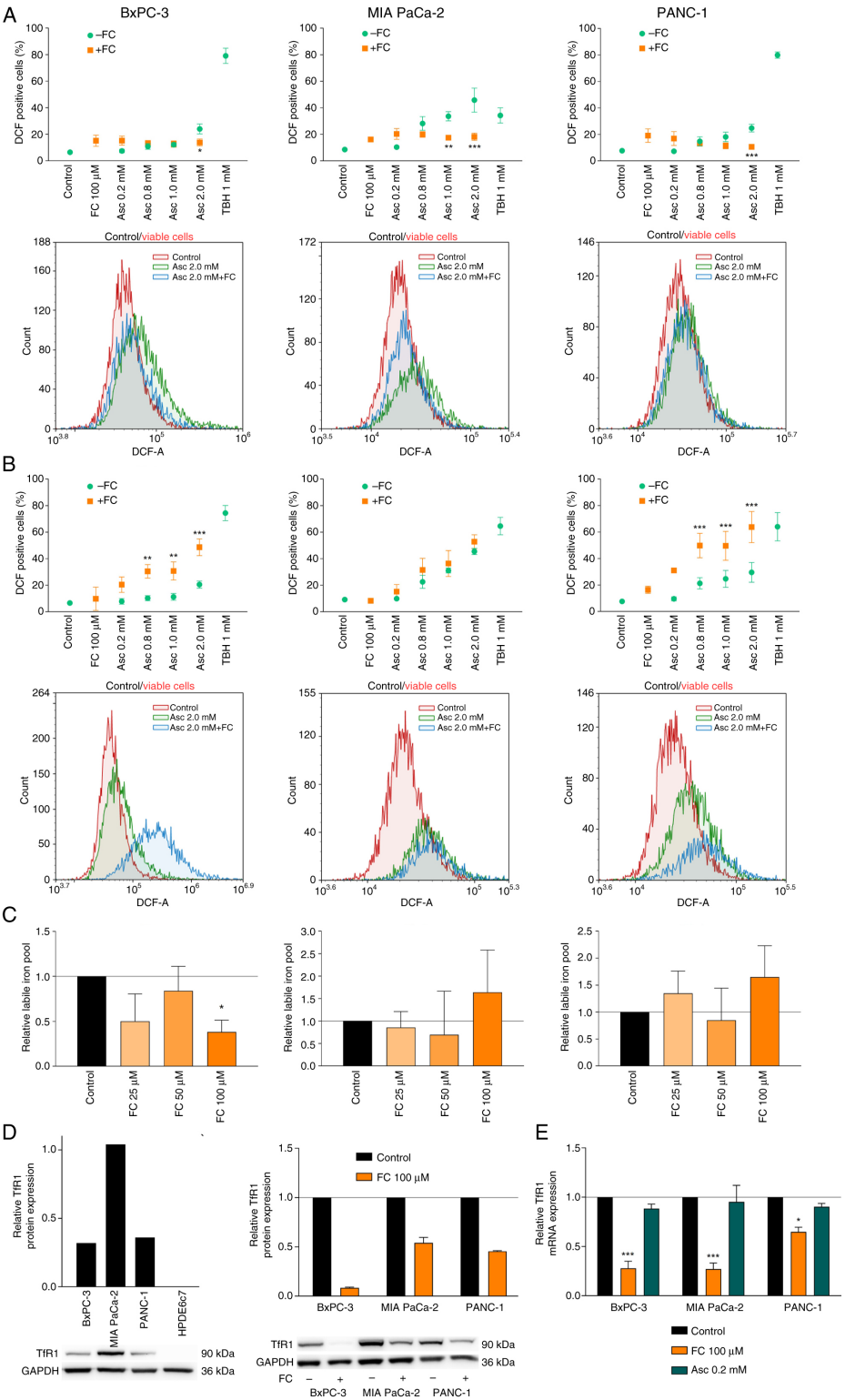

Figure 4. The influence of iron and TfR1 on the ascorbate effect in human pancreatic cancer cell lines. To investigate the effect of iron on ascorbate action, the three human pancreatic cancer cell lines BxPC-3, MIA PaCa-2, and PANC-1 were either incubated simultaneously for 6 h with ascorbate at different concentrations and 100 μM ferric chloride (FC) (A) or treated with ascorbate after 24 h preincubation with ferric chloride (B). The intracellular ROS levels were determined after treatment by flow cytometry using the DCFH-DA assay. The percentage of DCF-positive cells is shown as a measure of intracellular ROS accumulation. Statistically significant differences between the combination treatment with iron and ascorbate treatment alone are marked by asterisks. Three independent experiments were performed. The intracellular LIP after 24-h incubation with ferric chloride was determined by flow cytometry using the calcein AM assay (C). The relative labile iron pool is shown in relation to the untreated control. Three independent experiments were performed. The basal protein expression of TfR1 in the pancreatic cancer cell lines and the non-malignant pancreatic ductal epithelial cell line HPDE6c7 was determined by western blotting, as well as the influence of ferric chloride on TfR1 expression in the three pancreatic cancer cell lines (D). The western blot results were also analyzed densitometrically. A representative experiment is shown for basal expression. For TfR1 expression after iron treatment, two independent experiments were performed, a representative western blot is shown. The influence of the 24-h ferric chloride treatment as well as ascorbate treatment was additionally determined at the mRNA level by qPCR (E). Error bars represent the mean ± SD, statistical analysis with one-way ANOVA and subsequent Dunnett's multiple comparisons test, confidence interval 95%. *P≤0.05, **P≤0.01, and ***P≤0.001. Asc, ascorbate; DCFH-DA, dichlorodihydrofluorescein diacetate; DCF, dichlorofluorescein; FC, ferric chloride; LIP, labile iron pool; ROS, reactive oxygen species; TfR1, transferrin receptor 1.

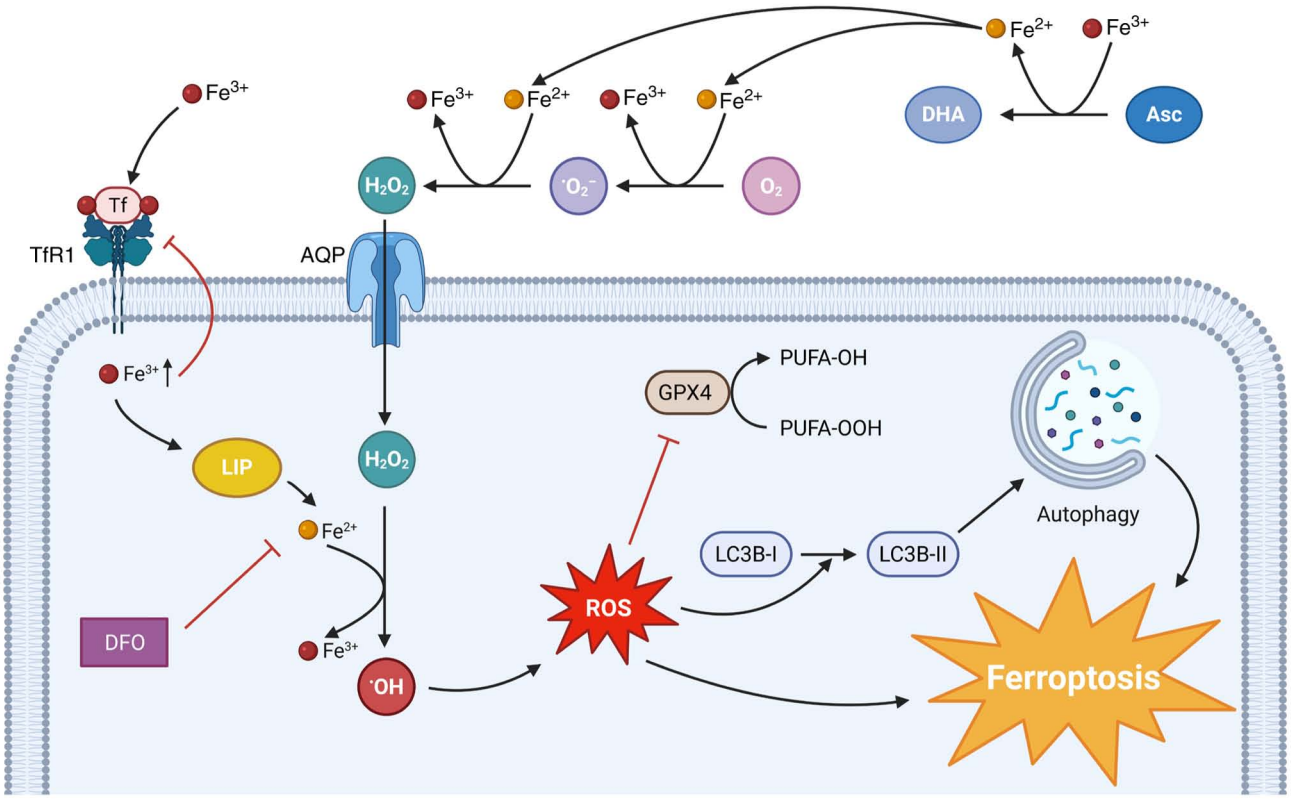

Figure 5. Hypothesized mechanism of ascorbate-induced cell death in pancreatic cancer cells. Asc is being oxidized outside the cell to DHA by ferric iron. This results in the accumulation of ferrous iron, which reacts with molecular oxygen and then with the superoxide radical anion to form hydrogen peroxide. Hydrogen peroxide enters the cancer cell via AQPs. Ferric iron itself enters the cell via TfR1, a process that is inhibited by intracellular iron accumulation and increased LIP. Once inside the cancer cell, hydrogen peroxide reacts with ferrous iron to form the hydroxyl radical, causing oxidative stress through ROS accumulation. This inhibits the antioxidant activity of GPX4, promotes autophagy, and finally induces ferroptotic cell death. Ferroptosis is inhibited by DFO. Asc, ascorbate; AQP, aquaporin; DFO, deferoxamine mesylate; DHA dehydroascorbic acid; GPX4, glutathione peroxidase 4; LIP, labile iron pool; PUFA, polyunsaturated fatty acids; ROS, reactive oxygen species; TfR1, transferrin receptor 1.

survival, a significant effect of the additional high-dose ascorbate administration was found on progression-free survival in the subpopulation of patients with KRAS-mutated metastatic colorectal cancer. However, these effects were observed without targeted iron supplementation.

It appears that iron supplementation is beneficial in patients without KRAS mutation, but detrimental in patients with KRAS mutation. If this is confirmed in further studies and/or in other tumor entities, this would mean that before using high-dose ascorbate in tumor patients, the KRAS status should be analyzed in order to identify a possible contraindication for the additional administration of iron or to increase the effectiveness of the therapy through a rational combination treatment.

It is surprising, however, that increased intracellular ROS formation was observed for the PANC-1 cells after 6 h of ascorbate treatment and prior preincubation with iron, with simultaneously reduced cytotoxicity of this form of combination treatment. However, since ascorbate treatment alone caused a low-threshold ROS induction in this cell line, it can be assumed that the cytotoxicity here is not solely due to ROS formation, but that other mechanisms also play a role, as summarized by Böttger *et al* (9).

The exact cell death mechanism by which high-dose ascorbate causes the death of tumor cells has not yet been conclusively clarified. Previous studies suggest that the form of cell death may vary between different tumor entities and depending on the concentration used (29). However, as summarized by Szarka *et al* (29), apoptotic cell death can be ruled out in most cases, which is presumably related to the fact that numerous tumor cells lose or greatly reduce their ability to undergo classical apoptosis during transformation (34). The present study also found minor indications of apoptosis after ascorbate treatment of human pancreatic cancer cells. In particular, caspase-3 activation, which is crucial for apoptosis, could not be detected in any of the cell lines analyzed using two different detection methods.

The current understanding of the antitumor mechanism of action of high-dose ascorbate as well as the data of this study suggest a key involvement of intracellular labile iron and the promotion of intracellular oxidative stress (35). Both factors are also crucial hallmarks of ferroptosis, which is why this form of cell death is discussed in connection with ascorbate (29). Nevertheless, signs of ferroptosis after ascorbate treatment have so far only been detected in oropharyngeal cancer and anaplastic thyroid cancer (36,37). In pancreatic carcinoma, there have been no studies on ferroptotic cell death after vitamin C treatment, but only indications that ascorbate can increase erastin-induced ferroptosis (38). In the present study, it could now be shown for the first time, to the best of our knowledge, that high-dose ascorbate triggers cell death in human pancreatic cancer cells, causing major signs of

ferroptosis. Interestingly, ferroptosis has increasingly become the focus of cancer therapy research in recent years, as various drugs that induce ferroptosis appear to be a promising option for overcoming drug resistance, especially in therapy-resistant tumors (39). High-dose ascorbate could therefore represent an effective alternative here, especially for second-line therapy.

Another important finding of the present study is the role of TfR1 in the application of high-dose ascorbate alone and in combination with iron. Interestingly, the cell line MIA PaCa-2, which was the most sensitive to vitamin C, shows by far the highest TfR1 expression, which could explain the high susceptibility of these cells: Namely, increased intracellular LIP would also increase intracellular ROS formation, as expected.

In line with this, treatment of the cells with $FeCl_3$ uniformly led to a significant, in some cases almost complete, decrease in TfR1 expression. As a result, the intracellular LIP of the cells could not be further increased or even decreased, which explains the partially reduced or unchanged ascorbate effect when combined with $FeCl_3$. The current understanding of the mechanism of action of high-dose ascorbate on PDAC cells, including the findings of the present study, is summarized in Fig. 5.

When trying to transfer this *in vitro* data onto the much more complex environment of a living organism, there are some difficulties that should be taken into consideration. One relevant point is that, in a clinical context, intravenous iron is usually administered in the form of iron-carbohydrate complexes, such as iron carboxymaltose, rather than the iron compounds used in most cell culture studies. These complexes are mainly taken up by macrophages in the liver, spleen, and bone marrow, and are continuously and in a controlled way delivered to transferrin, which distributes them throughout the body and to potential tumor tissue (40). The complexity of the pharmacokinetics of systemic iron supplementation makes it difficult to translate the *in vitro* data into a clinical context. For this reason, *in vivo* experiments with clinical iron compounds are needed to answer the remaining questions about transferring the results of the present study into a therapeutic approach.

Overall, it was shown for the first time that $FeCl_3$ does not synergize with high-dose ascorbate in the treatment of pancreatic cancer cells and may even reduce the antitumor effect of ascorbate. The explanation for this could be the reduced TfR1 expression after iron treatment, which results in reduced LIP. For this reason, when using high-dose ascorbate in tumor therapy, simultaneous iron administration should be carried out with caution and patients' iron levels should be monitored.

Acknowledgements

The authors would like to thank Mrs. Monika Schumacher (Technical Assistant, Department of Nutritional Biochemistry, Institute of Nutritional Sciences, University of Hohenheim) for her excellent technical support in conducting the experiments.

Funding

The present study was supported by the Dr. Hans Fritz Stiftung (grant no. 3140080501), the Ministry of Rural Affairs and Consumer Protection Baden-Wuerttemberg [grant no. AZ: 16 (34) 8402.43/0454 E], the PASCOE pharmazeutische Praeparate GmbH (grant nos. D.31.15100 and D.31.22506) and the Orthomol Pharmazeutische Vertriebs GmbH (grant no. 3140080701). Publishing fees supported by Funding Programme Open Access Publishing of University of Hohenheim.

Availability of data and materials

The data generated in the present study may be requested from the corresponding author.

Authors' contributions

AP conceptualized the study, curated data, conducted investigation, developed methodology, and visualized data. CL developed methodology and performed software analysis. HS, KD, KS, JS, SH, and LM curated data, conducted investigation and developed methodology. OR conceptualized the study and acquired funding. MB conceptualized and supervised the study and acquired funding. SV conceptualized and supervised the study, acquired funding, and conducted project administration. All authors wrote, reviewed, and edited the manuscript. All authors read and approved the final version of the manuscript. MB and SV confirm the authenticity of all the raw data.

Ethics approval and consent to participate

Not applicable.

Patient consent for publication

Not applicable.

Competing interests

The authors declare that they have no competing interests.

Use of artificial intelligence tools

During the preparation of this work, artificial intelligence tools were used to improve the readability and language of the manuscript or to generate images, and subsequently, the authors revised and edited the content produced by the artificial intelligence tools as necessary, taking full responsibility for the ultimate content of the present manuscript.

References

1. Siegel RL, Giaquinto AN and Jemal A: Cancer statistics, 2024. CA Cancer J Clin 74: 12-49, 2024.
2. Rahib L, Wehner MR, Matrisian LM and Nead KT: Estimated projection of US cancer incidence and death to 2040. JAMA Netw Open 4: e214708, 2021.
3. American Cancer Society: Cancer facts & figures. 2024. Available from: https://www.cancer.org/research/cancer-facts-statistics/all-cancer-facts-figures/2024-cancer-facts-figures.html.
4. National Cancer Institute: Cancer Stat Facts: Common Cancer Sites. 2025. Available from: https://seer.cancer.gov/statfacts/html/common.html.
5. Cameron E and Pauling L: Supplemental ascorbate in the supportive treatment of cancer: Prolongation of survival times in terminal human cancer. Proc Natl Acad Sci USA 73: 3685-3689, 1976.
6. Cameron E and Pauling L: Supplemental ascorbate in the supportive treatment of cancer: Reevaluation of prolongation of survival times in terminal human cancer. Proc Natl Acad Sci USA 75: 4538-4542, 1978.

7. Ou J, Zhu X, Lu Y, Zhao C, Zhang H, Wang X, Gui X, Wang J, Zhang X, Zhang T and Pang CLK: The safety and pharmacokinetics of high dose intravenous ascorbic acid synergy with modulated electrohyperthermia in Chinese patients with stage III-IV non-small cell lung cancer. Eur J Pharm Sci 109: 412-418, 2017.
8. Padayatty SJ, Sun H, Wang Y, Riordan HD, Hewitt SM, Katz A, Wesley RA and Levine M: Vitamin C pharmacokinetics: Implications for oral and intravenous use. Ann Intern Med 140: 533-537, 2004.
9. Böttger F, Vallés-Martí A, Cahn L and Jimenez CR: High-dose intravenous vitamin C, a promising multi-targeting agent in the treatment of cancer. J Exp Clin Cancer Res 40: 343, 2021.
10. Kim JH, Hwang S, Lee JH, Im SS and Son J: Vitamin C suppresses pancreatic carcinogenesis through the inhibition of both glucose metabolism and wnt signaling. Int J Mol Sci 23: 12249, 2022.
11. O'Leary BR, Alexander MS, Du J, Moose DL, Henry MD and Cullen JJ: Pharmacological ascorbate inhibits pancreatic cancer metastases via a peroxide-mediated mechanism. Sci Rep 10: 17649, 2020.
12. Bodeker KL, Smith BJ, Berg DJ, Chandrasekharan C, Sharif S, Fei N, Vollstedt S, Brown H, Chandler M, Lorack A, *et al*: A randomized trial of pharmacological ascorbate, gemcitabine, and nab-paclitaxel for metastatic pancreatic cancer. Redox Biol 77: 103375, 2024.
13. Alexander MS, Wilkes JG, Schroeder SR, Buettner GR, Wagner BA, Du J, Gibson-Corley K, O'Leary BR, Spitz DR, Buatti JM, *et al*: Pharmacologic ascorbate reduces radiation-induced normal tissue toxicity and enhances tumor radiosensitization in pancreatic cancer. Cancer Res 78: 6838-6851, 2018.
14. Chen P, Reed G, Jiang J, Wang Y, Sunega J, Dong R, Ma Y, Esparham A, Ferrell R, Levine M, *et al*: Pharmacokinetic evaluation of intravenous Vitamin C: A classic pharmacokinetic study. Clin Pharmacokinet 61: 1237-1249, 2022.
15. Polireddy K, Dong R, Reed G, Yu J, Chen P, Williamson S, Violet PC, Pessetto Z, Godwin AK, Fan F, *et al*: High dose parenteral ascorbate inhibited pancreatic cancer growth and metastasis: Mechanisms and a phase I/IIa study. Sci Rep 7: 17188, 2017.
16. Welsh JL, Wagner BA, van't Erve TJ, Zehr PS, Berg DJ, Halfdanarson TR, Yee NS, Bodeker KL, Du J, Roberts LJ II, *et al*: Pharmacological ascorbate with gemcitabine for the control of metastatic and node-positive pancreatic cancer (PACMAN): Results from a phase I clinical trial. Cancer Chemother Pharmacol 71: 765-775, 2013.
17. Fan D, Liu X, Shen Z, Wu P, Zhong L and Lin F: Cell signaling pathways based on vitamin C and their application in cancer therapy. Biomed Pharmacother 162: 114695, 2023.
18. Piotrowsky A, Burkard M, Schmieder H, Venturelli S, Renner O and Marongiu L: The therapeutic potential of vitamins A, C, and D in pancreatic cancer. Heliyon 11: e41598, 2025.
19. Du J, Cullen JJ and Buettner GR: Ascorbic acid: Chemistry, biology and the treatment of cancer. Biochim Biophys Acta 1826: 443-457, 2012.
20. González-Montero J, Chichiarelli S, Eufemi M, Altieri F, Saso L and Rodrigo R: Ascorbate as a bioactive compound in cancer therapy: The old classic strikes back. Molecules 27: 3818, 2022.
21. Schoenfeld JD, Alexander MS, Waldron TJ, Sibenaller ZA, Spitz DR, Buettner GR, Allen BG and Cullen JJ: Pharmacological ascorbate as a means of sensitizing cancer cells to Radio-chemotherapy while protecting normal tissue. Semin Radiat Oncol 29: 25-32, 2019.
22. Leischner C, Marongiu L, Piotrowsky A, Niessner H, Venturelli S, Burkard M and Renner O: Relevant membrane transport proteins as possible gatekeepers for effective pharmacological ascorbate treatment in cancer. Antioxidants (Basel) 12: 916, 2023.
23. Piotrowsky A, Burkard M, Hammerschmidt K, Ruple HK, Nonnenmacher P, Schumacher M, Leischner C, Berchtold S, Marongiu L, Kufer TA, *et al*: Analysis of High-dose ascorbate-induced cytotoxicity in human glioblastoma cells and the role of dehydroascorbic acid and iron. Antioxidants (Basel) 13: 1095, 2024.
24. Zhou L, Zhang L, Wang S, Zhao B, Lv H and Shang P: Labile iron affects pharmacological ascorbate-induced toxicity in osteosarcoma cell lines. Free Radic Res 54: 385-396, 2020.
25. Schoenfeld JD, Sibenaller ZA, Mapuskar KA, Wagner BA, Cramer-Morales KL, Furqan M, Sandhu S, Carlisle TL, Smith MC, Abu Hejleh T, *et al*: $O_2^{\cdot-}$- and H2O2-mediated disruption of fe metabolism causes the differential susceptibility of NSCLC and GBM cancer cells to pharmacological ascorbate. Cancer Cell 31: 487-500.e8, 2017.
26. Du J, Wagner BA, Buettner GR and Cullen JJ: Role of labile iron in the toxicity of pharmacological ascorbate. Free Radic Biol Med 84: 289-295, 2015.
27. Livak KJ and Schmittgen TD: Analysis of relative gene expression data using real-time quantitative PCR and the 2(-Delta Delta C(T)) method. Methods 25: 402-408, 2001.
28. Burkard M, Niessner H, Leischner C, Piotrowsky A, Renner O, Marongiu L, Lauer UM, Busch C, Sinnberg T and Venturelli S: High-dose ascorbate in combination with Anti-PD1 checkpoint inhibition as treatment option for malignant melanoma. Cells 12: 254, 2023.
29. Szarka A, Kapuy O, Lőrincz T and Bánhegyi G: Vitamin C and cell death. Antioxid Redox Signal 34: 831-844, 2021.
30. Chen X, Comish PB, Tang D and Kang R: Characteristics and biomarkers of ferroptosis. Front Cell Dev Biol 9: 637162, 2021.
31. Brandt KE, Falls KC, Schoenfeld JD, Rodman SN, Gu Z, Zhan F, Cullen JJ, Wagner BA, Buettner GR, Allen BG, *et al*: Augmentation of intracellular iron using iron sucrose enhances the toxicity of pharmacological ascorbate in colon cancer cells. Redox Biol 14: 82-87, 2018.
32. Deme S, Ramezani I, Coulter J, Paller C and Bressler J: Effects of hypoxia and iron on ascorbic acid-mediated cytotoxicity in prostate cancer cell lines. Toxicol Appl Pharmacol 497: 117259, 2025.
33. Wang F, He MM, Xiao J, Zhang YQ, Yuan XL, Fang WJ, Zhang Y, Wang W, Hu XH, Ma ZG, *et al*: A randomized, open-label, multicenter, phase 3 study of high-dose Vitamin C Plus FOLFOX ± bevacizumab versus FOLFOX ± bevacizumab in unresectable untreated metastatic colorectal cancer (VITALITY study). Clin Cancer Res 28: 4232-4239, 2022.
34. Mohammad RM, Muqbil I, Lowe L, Yedjou C, Hsu HY, Lin LT, Siegelin MD, Fimognari C, Kumar NB, Dou QP, *et al*: Broad targeting of resistance to apoptosis in cancer. Semin Cancer Biol 35 (Suppl(0)): S78-S103, 2015.
35. Renner O, Burkard M, Michels H, Vollbracht C, Sinnberg T and Venturelli S: Parenteral high-dose ascorbate-A possible approach for the treatment of glioblastoma (Review). Int J Oncol 58: 35, 2021.
36. Wu K, Liu L, Wu Z, Huang Q, Zhou L, Xie R and Wang M: Ascorbic acid induces ferroptosis via STAT3/GPX4 signaling in oropharyngeal cancer. Free Radic Res 58: 117-129, 2024.
37. Wang X, Xu S, Zhang L, Cheng X, Yu H, Bao J and Lu R: Vitamin C induces ferroptosis in anaplastic thyroid cancer cells by ferritinophagy activation. Biochem Biophys Res Commun 551: 46-53, 2021.
38. Liu Y, Huang P, Li Z, Xu C, Wang H, Jia B, Gong A and Xu M: Vitamin C sensitizes pancreatic cancer cells to erastin-induced ferroptosis by activating the AMPK/Nrf2/HMOX1 pathway. Oxid Med Cell Longev 2022: 5361241, 2022.
39. Zhang C, Liu X, Jin S, Chen Y and Guo R: Ferroptosis in cancer therapy: A novel approach to reversing drug resistance. Mol Cancer 21: 47, 2022.
40. Schaefer B, Meindl E, Wagner S, Tilg H and Zoller H: Intravenous iron supplementation therapy. Mol Aspects Med 75: 100862, 2020.